Fusion of propagation observations and numerical weather prediction via warping functions

Ted Rogers, and Chelsea Mediavilla
SPAWAR Systems Center Pacific
trogers@spawar.navy.mil

I. Introduction

The inverse problem in trans-horizon electromagnetic (EM) propagation has been solved by mapping modeled refractive environments ($\mathcal{M}$'s) into the space of observed propagation $\mathbf{d}$ and selecting the best $\mathcal{M}$ based on goodness-of-fit. Up to the present, parametric *ad hoc* refractivity models have been used, e.g., [2], [3], [4]. We modify this approach by using an *a priori* $\mathcal{M}$ from numerical weather prediction (NWP) and solving for warping coefficients (ν's) within a 2-dimensional variational (2DVAR) analysis. The warping (or mapping) is

$$\mathcal{M}_a, \nu \xrightarrow{g(\cdot,\nu)} \mathcal{M} \xrightarrow{f(\cdot)} \mathbf{d} \tag{1}$$

where $\mathcal{M}_a$ is the *a priori* (e.g. NWP) refractivity fields, our $g(\cdot)$ is a composition of functions that maps $\mathcal{M}_a$ into the a new a warped $\mathcal{M}$, ν is a vector of warping coefficients, and $f(\cdot)$ is the electromagnetic propagation model that maps $\mathcal{M}$ [1] into the space of observations $\mathbf{d}$. The 2DVAR is implemented

$$\nu = \underset{\nu}{\arg\min} \left[\nu^T \mathbf{B}_\nu{}^{-1} \nu + (\mathbf{d} - \mathbf{H}g(\mathbf{x}_b, \nu))^T \mathbf{R}^{-1} (\mathbf{d} - \mathbf{H}g(\mathbf{x}_b, \nu)\right] \tag{2}$$

where the $\mathbf{B}_\nu$ is the background covariance in the space of ν, $\mathbf{R}$ is the observation error covariance, $\mathbf{H}$ selects the elements of $g(\mathbf{x}_b, \nu)$ corresponding to the measurements $\mathbf{d}$. $\mathbf{B}_\nu$ and $\mathbf{R}$ are conventionally defined

$$\mathbf{B}_\nu = \langle \nu \nu^T \rangle \tag{3}$$

$$\mathbf{R} = \langle (\mathbf{H}g(\mathbf{x}_b, \nu) - \langle \mathrm{d} \rangle) (\mathbf{H}g(\mathbf{x}_b, \nu) - \langle \mathrm{d} \rangle)^T \rangle \tag{4}$$

and $g(\cdot, \nu)$ is engineered such that $\nu = 0$ corresponds to un-warped values. In this initial proof-of-concept, illustrative *ad hoc* values of $\mathbf{B}_\nu$ and $\mathbf{R}$ are utilized.

II. Warping functions

The warping functions employed are:

1) $g_1(\cdot, \nu_1)$ strengthens / weakens gradients more negative than 0.128 M-units per meter by a multiplicative factor of $\nu_1 + 1$.
2) $g_2(\cdot, \nu_2)$ vertically shifts the profiles by ν_2 meters after a 0.128 M-units per meter gradient for negative heights.
3) $g_3(\cdot, \nu_3)$ modifies the evaporation duct.

Examples are shown in Fig. 1.

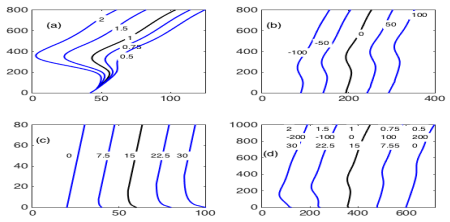

Fig. 1. Demonstration of operators where $\nu = [0, 0, 0]'$ corresponds to no warping. (a) Strengthening/Weakening $g_1(\cdot, \nu_1)$ for values of $\nu_1 = [1, 0.5, 0, -0.25, -0.5]$. (b) Vertical Displacement $g_2(\cdot, \nu_2)$ operator illustrated for shifts of -100m to 100m; zero-shift corresponds to profile unmodified by shift operator. (c) Evaporation Duct $g_3(\cdot, \nu_3)$ Operator. (d) Output of different realizations of ν. x-axis is modified refractivity with affine offsets and y-axis is height above surface; varied as needed to illustrate behavior.

III. Example from CASPER West experiment

Figure 2 is an illustrative simulation utilizing an archived NWP volume. Simulated truth was

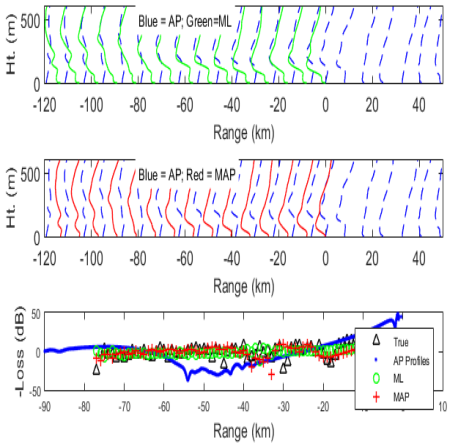

Fig. 2. Simulation using AREPSsocal volume. 1st (upper) plot: Synthetic ground truth refractivity fields (top row; Black). NWP starter field (Blue) chosen because it would likely require significant adjustment. 2nd plot: Refractivity fields inverted without using prior statistics in Green (i.e., the maximum likelihood estimate) are overlaid on synthetic true (Black). 3rd plot: Refractivity fields inverted using prior statistics (i.e., the maximum *a posteriori* estimator) in Red are again overlaid on synthetic true (Black). 4th plot: Propagation loss as a function of range corresponding to refractivity fields shown above, using same color scheme where the triangles represent the observed data.

chosen to be a set of profiles corresponding to a surface based duct. The simulated background corresponds to an elevated duct. The simulated-true environment was input to the Advanced Propagation Model (APM) [1] for 10-meter transmitter and receiver heights, a frequency of 3.0 GHz and a smooth surface (i.e., over-water with no wind) to generate simulated propagation loss (black in the 4th plot; underneath the green).

IV. Summary

Warping holds promise in avoiding the lossy or ambiguous mapping between the space of NWP and a parametric refractivity models. Whereas most data assimilation methods correct amplitude, warping corrects location errors, hence is less constrained (or restrictive) in how errors are corrected. By exploiting NWP's ability and the ability to correct location errors, it may reduce the degrees of

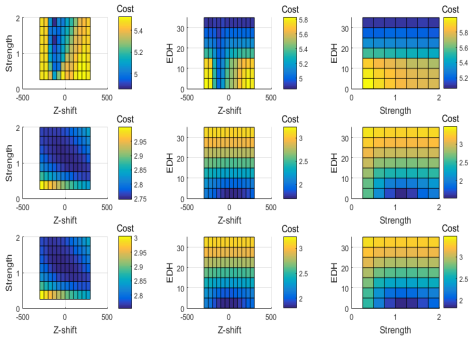

Fig. 3. Cost functions associated with Figure 2. Upper row corresponds to "without prior", i.e., using only the observation quadratic in Equation 2. Middle row corresponds to the cost of the prior by itself. Bottom row corresponds to using both terms on the right-hand-side of Equation 2.

freedom required for obtaining a level of goodness from the inversion / assimilation process.

References

[1] A. Barrios and W. L. Patterson, "Advanced propagation model (APM) ver. 1.3.1 computer software configuration item (CSCI) documents," SPAWAR Systems Center, San Diego, CA, Tech. Rep. Tech. Doc. 3145, 2002.

[2] L. T. Rogers, "Remote sensing of evaporation ducts using shf propagation measurements," no. AGARD-CP-582. Advisory Group for Aerospace Research and Development (AGARD), April 1996, pp. 48.1– 48.9.

[3] ——, "Likelihood estimation of tropospheric duct parameters from horizontal propagation measurements," *Radio Science*, vol. 32, no. 1, pp. 79–92, 1997.

[4] F. Vasileios and C. Earls, "Inverting for maritime environments using proper orthogonal bases from sparsely sampled electromagnetic propagation data," *IEEE Trans. Geosci. Remote Sens.*, vol. 54, no. 12, pp. 7166–7176, Aug. 2016.